



# Dispersive Liquid-Liquid Microextraction Based on Solidification of Floating Organic Drop with Central Composite Design for the Spectrofluorometric Determination of Naproxen

Maryam Shirinnejad<sup>1</sup> · Amir H. M. Sarrafi<sup>1</sup>

Received: 1 June 2019 / Accepted: 8 July 2019 / Published online: 22 July 2019  
© Springer Science+Business Media, LLC, part of Springer Nature 2019

## Abstract

A quick, simple and efficient method for extraction, preconcentration, and determination of naproxen in water and plasma specimens with acceptable recovery by dispersive liquid-liquid microextraction based on solidified floating organic drop with spectrofluorimetry is presented. Various parameters affecting the extraction efficiency are optimized by the Central Composite Design. Moreover, under optimal conditions (120  $\mu$ L 1-Undecanol with 1 mL Ethanol, pH = 3.5, 2 mL KCl 10% solution), the calibration curve was linear in the range 10.0–120.0 ng/mL. Finally, for naproxen, the detection limit was 2.4 ng/mL.

**Keywords** Naproxen · DLLME-SFO · Spectrofluorimetry · Central composite design

## Introduction

Naproxen, [(S) -2- (6-methoxy-2-naphthyl) propionic acid] (NAP) non-steroidal anti-inflammatory drug (NSAID) is widely used to treat pain-related diseases like rheumatic diseases in humans. The use of NSAIDs can reduce the risk of developing Alzheimer's disease, leading to an increase in human life expectancy. However, long-term use of NSAIDs can cause some toxic effects, such as gastrointestinal bleeding, intestinal ulcer, aplastic anemia, and blockage of platelet aggregation [1]. Although the concentration of drugs in environmental samples is low, it can be sufficient to produce toxic effects [2]. Due to the widespread use of these compounds and their entry into the water and their remaining residues in human serum, developing a sensitive analytical method for controlling them in blood and water samples is an important issue. Direct use of analytical techniques is limited to determining the analyte in complex matrices, despite the many interference components associated with low concentrations of analyte in

real samples. Therefore, the sample preparation stage is often needed before doing the measurement. Several methods for measuring small amounts of NAP have been used based on analytical techniques including Gas Chromatography-Mass Spectrometry (GC-MS) [2], Spectrofluorimetry [3–7], High-Performance Liquid Chromatography (HPLC-UV) [8–11] and Voltammetry [12, 13] and electrochemical methods [14–17].

Recent research activities focused on the development of efficient, economical and miniature prototype preparation methods. As a result, the development of Dispersive liquid-liquid microextraction (DLLME) has been considered among other methods. The DLLME method was introduced on the basis of a three-component solvent system such as liquid-liquid homogeneous extraction and cloud-point extraction [18]. Of course, the main drawback of this method is Isolation of low solvent extraction amount. In recent years, the DLLME method has been used in different areas of analytical chemistry and some proceedings have been taken to improve this method [19–23]. Leung and Huang introduced a new method of dispersion liquid-liquid microextraction based on solidifying floating organic droplet (DLLME-SFO) [24]. In this method, solvents with a lower density of water and less toxicity are used as a liquid extractor at room temperature. In this method, the extraction is performed on the basis of the classic DLLME, with an extraction solvent together with a dispersion solvent, immiscible with the sample solution and the extraction solvent, with the exception that the

✉ Amir H. M. Sarrafi  
A\_mohsensarafi@iauctb.ac.ir

<sup>1</sup> Research Laboratory of Analytical Chemistry, Department of Chemistry, Faculty of Science, Islamic Azad University Central Tehran Branch, Tehran, Iran

extractor solvent solidifies at relatively high temperatures and therefore its separation from our sample environments is easy. [25, 26]

Chemometrics has achieved major assessment and progress in the analytical chemistry field. The use of Chemometrics helps the analyzer to improve experimental methods. Statistical and mathematical techniques used for develop, improve, and optimize a process are known as the RSM method. Experimental design, in addition to minimizing the number of experiments, has high efficiency for operating conditions and minimum cost, while providing a good knowledge of the interactions of variables. The statistical analysis describes the relationships between effective variables (independent variables) and dependent variables (responses) [27–29]. The experimental design has found many applications in the DLLME approach [30]. In this study, the method of dispersive liquid-liquid micro-extraction based on solidifying floating organic drop (DLLME-SFO) was used to pre-concentration and to the separation of ultra-trace NAP and to measure it by spectrofluorimetry. The central composite design method (CCD) was used to investigate the effects of significant operational parameters such as pH, extraction solvent amount and sample ionic strength, and find the best combination of variables. The second-order polynomial regression equation provides an excellent explanation for the response (the intensity of fluorescence emission in excitation wavelength) and independent parameters. Finally, an optimized method for measuring NAP was used in water and blood serum samples.

## Experimental

### Materials

Naproxen (NAP) was prepared from Sigma-Aldrich. 1-Undecanol and 1-Dodecanol, Acetonitrile, Methanol, Acetone, Ethanol, Sodium hydroxide, Potassium Chloride, Phosphoric Acid, Acetic Acid and Boric Acid were prepared from Merck Co. All materials used were analytical grade purity and were used without any re-purification. Double-distilled water (DDW) was utilized in all experiments.

### Instruments and Software

For spectrophotometric measurements, the Perkin-Elmer Lambda 25 was used. The fluorescence spectra were obtained with a Perkin-Elmer LS 55 spectrophotometer with a width of 5 nm of excitation and emission slits. Sonorex RK100 ultrasonic bath and Hettich D-78532 centrifuge were used during the tests. The Denver UB-10 and Hamilton microsyringe 1 mL were used during the experiments. Design Expert 10.0.1.0 and Minitab 17.3.1 were used for experimental design and statistics tests respectively.

## Sample Preparations

A standard solution of 1 mM NAP was prepared in double-distilled water and stored for testing in the dark and 4 °C. Buffer solutions of Britton-Robinson were prepared with the aid of suitable amounts of acetic acid, phosphoric acid, and boric acid. Damavand mineral water samples and tap water is filtered by 0.45 µm filter and used without any preparation. Human plasma samples were obtained from the Blood Transfusion Organization of Iran. 3 mL of the plasma sample

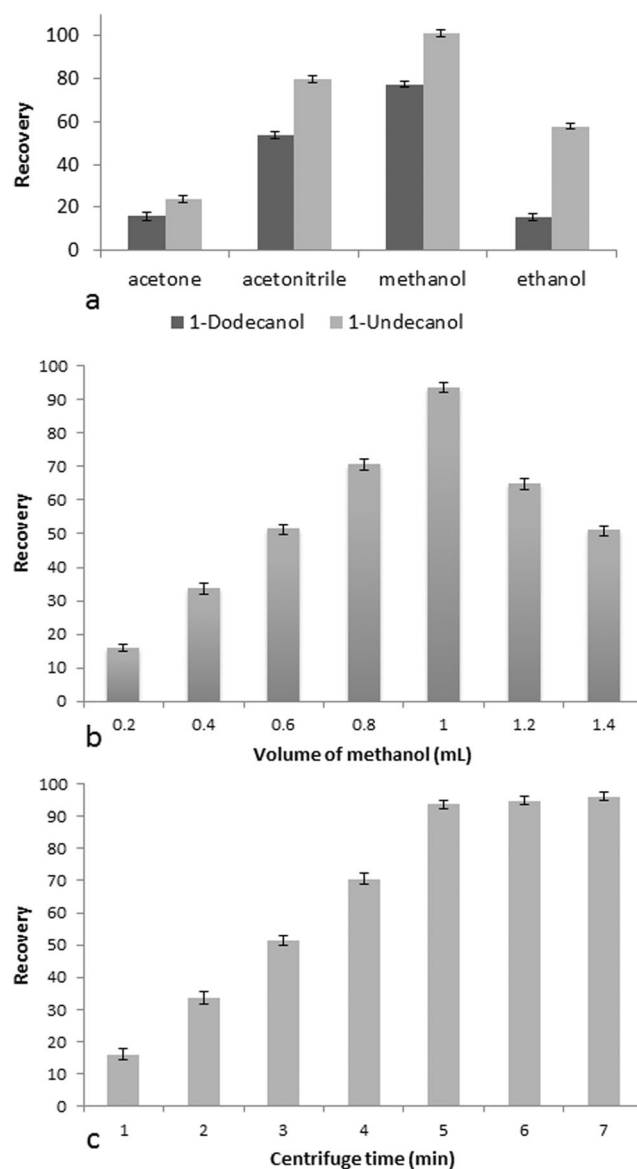


**Fig. 1** (a) Selection of the extraction-disperser mixed solvents. DLLME-SFO conditions: NAP, 120 µg/L; extractant, 120 µL; disperser, 1 mL; pH, 3.5; centrifuge, 5 min in 5000 rpm. (b) Selection of the disperser solvent volume. DLLME-SFO conditions: NAP, 120 µg/L; 1-Undecanol, 120 µL; disperser, methanol; pH, 3.5; centrifuge, 5 min in 5000 rpm. (c) Selection of centrifuge time. DLLME-SFO conditions: NAP, 120 µg/L; extractant, 120 µL; disperser, 1 mL; pH, 3.5; centrifuge, 5000 rpm

was mixed with 3 mL of acetonitrile to remove the proteins and then centrifuged for 30 min at 8000 rpm. After centrifugation, the upper layer was collected and the remaining acetonitrile evaporated using nitrogen gas flow and stored for further use at 4 °C.

### Assay Procedure

Under optimum conditions, pH of 15 mL of the sample containing different concentrations of naproxen in conical centrifuge tube was adjusted to 3.5. Then 0.5 mL 10% potassium chloride solution was added. With the addition of 120 µL 1-Undecanol and 1 mL of methanol with Hamilton microsyringe, the solution was cloudy. Sample tubes were centrifuged at 5,000 rpm for 6 min and placed in an ice bath for 10 min. After this time, the extracted solid drop solvent was separated from the sample. 2 mL of acetonitrile was added to the extraction solvent and the spectra of the samples were recorded at a 330 nm excitation wavelength in the range of 345 to 500 nm. All experiments were repeated three times.

### Experimental Design

In the present work, the researcher used the dependence of the emission intensity of NAP on three variables, pH of the sample solution (2 to 6), the KCl 10% volume (ionic strength of the sample solution, 0-1 mL) and the 1-Undecanol volume (40-200 µL). The CCD was used to examine simultaneously the optimal conditions, the main factors and the interactions between them. Initial screening studies were conducted based on a literature review to select the appropriate range of selected variables. Then, factors were designed in five levels, 20 runs (6 runs axial, 8 cubic runs (complete 8 factorial complete design) and 6 replicated central points with  $\alpha = 2$ ). Finally, the

relationship between the three variables was estimated by a quadratic polynomial model.

$$Y = \beta_0 + \sum_{i=1}^K \beta_i X_i + \sum_{i=1}^k \sum_{j=i+1}^K \beta_{ij} X_i X_j + \sum_{i=1}^K \beta_{ii} X_i^2 \quad (1)$$

Where  $X_i$  and  $X_j$  are the variables,  $\beta_0$  is the model constant,  $\beta_i$  is the linear coefficient,  $\beta_{ij}$  is the interaction coefficient between the variables and  $\beta_{ii}$  is the nonlinear coefficient of the second order of the main variables. Analysis of variance (ANOVA) was used to obtain the statistical significance of each factor, the interaction between them and the adequacy of the developed regression model. Due to the effect of other experimental parameters, the type of extraction solvent, the distribution solvent type and volume, the time and speed of centrifugation were optimized by changing a parameter in time and maintaining the remaining parameters.

## Results and Discussions

### Optimization Process

#### Type of Extraction and Disperser Solvents

The extraction solvent nature plays an important role in extracting naproxen from the sample. The extraction solvent must have the high extraction potential of the analyte, indiscriminately with water, which are a density below water and melt at room temperature. Dispersion solvent also plays an important role. Dispersion solvent must be embedded with water and extraction solvent so that, after increasing it to the solution, it can disperse the extraction solvent into very fine droplets in the sample solution. This feature creates a higher contact level between the extraction solvent and the aquatic

**Table 1** ANOVA test results on experimental data based on quadratic polynomial model

| Source                        | Sum of Squares | df | Mean Square | F Value | p value Prob > F |                 |
|-------------------------------|----------------|----|-------------|---------|------------------|-----------------|
| Model                         | 2.061E-005     | 6  | 3.435E-006  | 617.64  | < 0.0001         | Significant     |
| X <sub>1</sub> -pH            | 9.268E-006     | 1  | 9.268E-006  | 1666.64 | < 0.0001         |                 |
| X <sub>2</sub> -Salt-%10      | 9.110E-008     | 1  | 9.110E-008  | 16.38   | 0.0014           |                 |
| X <sub>3</sub> -Undecanol     | 1.082E-006     | 1  | 1.082E-006  | 194.56  | < 0.0001         |                 |
| X <sub>1</sub> X <sub>3</sub> | 3.753E-007     | 1  | 3.753E-007  | 67.49   | < 0.0001         |                 |
| X <sub>1</sub> <sup>2</sup>   | 9.744E-006     | 1  | 9.744E-006  | 1752.21 | < 0.0001         |                 |
| X <sub>3</sub> <sup>2</sup>   | 1.132E-007     | 1  | 1.132E-007  | 20.36   | 0.0006           |                 |
| Residual                      | 7.229E-008     | 13 | 5.561E-009  |         |                  |                 |
| Lack of Fit                   | 3.840E-008     | 8  | 4.800E-009  | 0.71    | 0.6840           | not significant |
| R <sup>2</sup>                | 0.9965         |    |             |         |                  |                 |
| Adjusted-R <sup>2</sup>       | 0.9849         |    |             |         |                  |                 |
| Adequate Precision            | 95.481         |    |             |         |                  |                 |

environment. Thus, the extraction equilibrium results quickly and in higher yields. In this study, six solvents were examined, 1-Undecanol, and 1-Dodecanol as extraction solvents, ethanol, methanol, acetonitrile, and acetone as dispersion solvents. In order to detect the best combination of extraction solvent and dispersion solvent, a series of experiments were carried out for different combinations of extraction and dispersion solvent under the same conditions. The results are presented in Fig. 1a.

The results show that the 1-Undecanol and methanol mixtures provide the highest extraction efficiency. At this stage, experiments were carried out with the combination of 1-Undecanol extraction solvent and different methanol values

in the range of 0.2–1.4 mL. The results are presented in Fig. 1b. Based on the results, 1 mL of methanol was selected.

### Centrifuge Time and Rate

A centrifuge is used to better separation of extraction solvent from the aqueous sample. In order to optimize these two parameters, experiments were carried out in identical conditions for the amount of the NAP, the type and amount of solvent, the type and amount of extraction solvent in 5000 rpm with variable centrifuge time. The results are presented in Fig. 1c. As shown, rising by centrifuge time from 1 to 5 min caused improved recovery, but after 5 min had no significant effect.

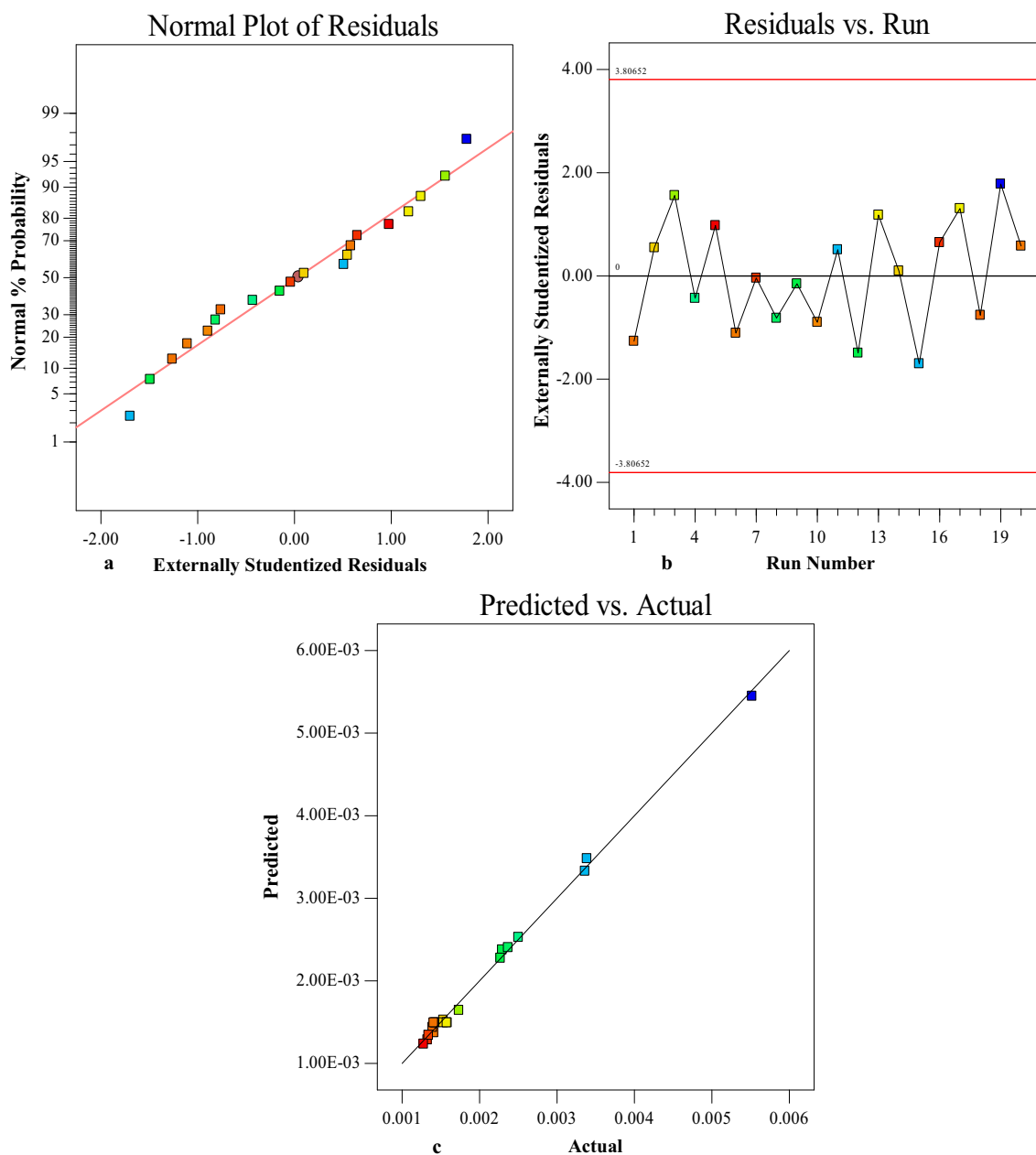


**Fig.2** (a) Normal probability plot, (b) A plot of the externally studentized residuals vs run number, (c) The predicted response vs. the observed response

### CCD Optimization

Based on CCD-based experiments, the effects of variables, sample solution pH, the KCl 10% volume added and the 1-Undecanol volume of was evaluated. According to experimental data, a quadratic polynomial

model was used to describe the response variable (emission intensity of 351 nm at the excitation wavelength of 330 nm) and the interaction between variables. Normally distributed data are required for statistical analysis tools such as control charts and analysis of variance (ANOVA). Using a parametric statistical test

**Fig. 3** 3D Surface Response and Contour Plot using the central composite design obtained by plotting: (a) pH vs. mL KCl 10%, (b) pH vs. 1-Undecanol  $\mu\text{L}$ , (c) mL KCl 10% vs. 1-Undecanol  $\mu\text{L}$

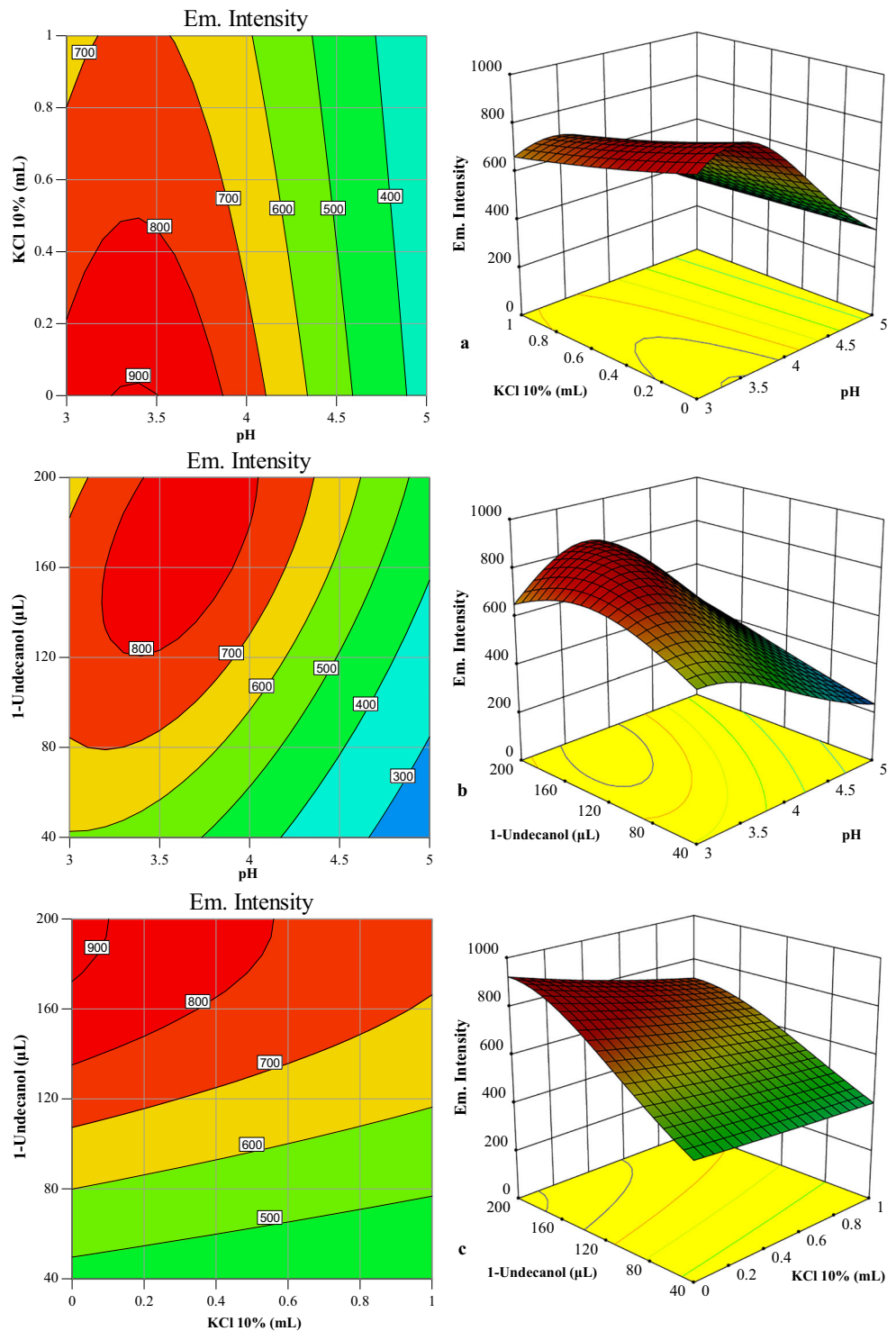


**Table 2** Comparison of developed method with other methods for determination of NAP

| Method   | Sample                 | LOD ng/mL | Linear range ng/mL | Ref.      |
|--|------------------------|-----------|--------------------|-----------|
| HF-SPME-HPLC <sup>a</sup>                                | Water                  | 0.01      | 0.03–500           | [10]      |
| VAI-DLLME-HPLC <sup>b</sup>                              | Plasma                 | 0.32      | 1–1000             | [8]       |
| HPLC   | Plasma                 | 10        | 15–40              | [9]       |
| PANI-Fe <sub>3</sub> O <sub>4</sub> -SPE-FL <sup>c</sup> | Human urine and plasma | 17        | 40–1000            | [3]       |
| DLLME-SFO-FL   | Water and plasma       | 2.4       | 10.0–120.0         | This work |

<sup>a</sup> Hollow fiber solid phase microextraction

<sup>b</sup> Vortex-assisted inverted dispersive liquid-liquid microextraction

<sup>c</sup> Magnetic nanofiber polyaniline nanocomposite-solid phase extraction

(such as regression or ANOVA) on abnormal data can lead to misleading results. Data transfer and, in particular, the transfer of Box-Cox power is one of these corrective actions that can help to create normal data. George Box and David Cox have developed a method to identify an appropriate index ( $\lambda$ ) for use in converting data into a normal shape. The lambda value represents the type of transfer that must be applied to all data. To do this, the Box-Cox power conversion from  $\lambda = -3$  to  $\lambda = +3$  is searched to find the optimal value [31]. In this case, this transfer is defined as:

$$T(Y) = (Y^\lambda - 1) / \lambda \quad (2)$$

Where  $Y$  is the response variable and  $\lambda$  is the transmission parameter. Box-Cox Plot (plotting the sum of squares of the unclassified remainders by the model versus  $\lambda$ ) is a tool that helps us determine the most appropriate power variation for applying to response data. In this research, after a quadratic polynomial regression on the initial response data, the Box-Cox plot showed that the transmission of the response data  $I_e$  (emission intensity) to  $1/I_e$  leads to better modeling. Therefore, the second-order quadratic polynomial regression modeling was repeated to describe relationships between the transmitted response variable and the variables. ANOVA test

was used to test the validity of the model, the effect of the main variables, and the interaction between them, the nonlinear effect of the main variables and the adequacy of the developed regression model. The importance of each factor with  $P$  value  $< 0.05$  is determined and the validity of the proposed model is measured by the coefficient of determination ( $R^2$ , Adjusted- $R^2$ ). The results of the ANOVA test are presented in Table 1.

According to experimental data, a quadratic polynomial model was used to describe the relationship between variables as Eq. (3):

$$\begin{aligned} (1/I_e) = & +6.79888E-003 - 3.45367E-003 * X_1 \\ & + 3.01822E-004 * X_2 \\ & + 5.32648E-006 * X_3 - 5.41496E-006 * X_1 X_3 \\ & + 6.08069E-004 * X_1^2 + 4.09679E-008 * X_3^2 \quad (3) \end{aligned}$$

$R^2 = 0.9965$  and Adjusted- $R^2 = 0.9849$  show a great relationship between empirical values and a fitted model and display model efficiency to predict the response. Based on ANOVA data, F-value (617.64) and  $P$  value ( $< 0.0001$ ) indicate the significance of the developed model. Adequate Precision = 95.48, a measure of the experimental signal-to-

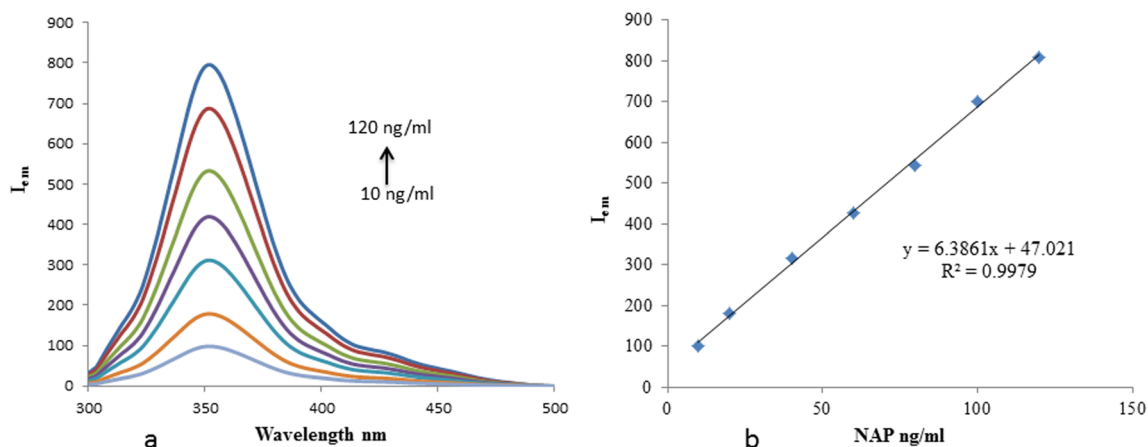


**Fig. 4** (a) Fluorescence emission spectra of NAP after microextraction in optimum conditions, (b)  $I_e$  vs. NAP (10–120 ng/mL)

**Table 3** Results of determining NAP in real sample

| Sample        | Added NAP ng/mL |  | Found NAP±RSD% ng/mL<br>N.D | Rec.%<br>– |
|---------------|-----------------|--|-----------------------------|------------|
|               | 0               |  |                             |            |
| DDW           | 40.0            |  | 40.1 ± 1.5                  | 100.3      |
|               | 100.0           |  | 99.3 ± 1.2                  | 99.3       |
| Mineral Water | 40.0            |  | 40.0 ± 1.7                  | 100.0      |
|               | 100.0           |  | 98.1 ± 1.6                  | 98.1       |
| Tap Water     | 40.0            |  | 38.4 ± 2.5                  | 95.9       |
|               | 100.0           |  | 96.1 ± 1.9                  | 96.1       |
| Plasma        | 40.0            |  | 37.9 ± 3.1                  | 94.8       |
|               | 100.0           |  | 95.3 ± 2.4                  | 95.3       |

noise ratio that compares the range of the predicted responses at the design points to the average variance of the prediction also indicates the adequacy of modeling. The P value for Lack of fit (0.6840) suggests that lack of fit of the fitted model is not significant. The normal probability plot (Fig. 2a) shows that the points follow a normal distribution. The studentized residual plot against the Run number (Fig. 2b) was also controlled. The random pattern of the residuals indicates the high suitability of the model and its non-dependence on the order of runs. Figure 2c shows predicted responses versus the observed data. Most results are close to the right line, which indicates a good relationship between the actual data and the fitted model.

In the next step, to view the effects of the variables separately and interaction between them in the emission intensity, 3D surface diagrams, and Contour plots were used. Responses were plotted versus two important variables, while the other factor was fixed at its central level. The objective of the response surface is to find the optimal values of the factors in the case of maximum emission intensity (Fig. 3a-c).

As shown in Fig. 3a and b, the emission intensity increases in the pH range (3–4). With respect to  $pK_a = 4.15$  NAP [30], the maximum amount of NAP extracted in this pH range was expected by 1-Undecanol. The ionic strength in liquid phase extraction methods can have a dual effect on extraction efficiency. Increasing the ionic strength of the sample reduces the

solubility of organic analytes in the aqueous phase due to the salting out effect and, in some cases, increases the salting-in effect. In Fig. 3a and c, the initial increase in ionic strength of the solution increases the extraction efficiency and thus increases the emission intensity, but by further increasing the ionic strength, decreases the extraction efficiency and therefore decreases the emission intensity. As shown in Fig. 3b and c, amount of 1-Undecanol in the range of 100–200  $\mu\text{L}$  results in higher efficiency and enhanced emission intensity. Finally, the developed model presented the optimal parameters of the extraction process at  $\text{pH} = 3.5$ , the KCl 10% volume equal to 2 mL, and the volume of the 1-Undecanol solvent 120  $\mu\text{L}$ . Experiments for 80.0 ng/mL NAP were repeated with 1 mL of methanol (dispersion solvent), centrifuge rate 5000 rpm and, centrifuge time 5 min, and the result was  $542.17 \pm 1.81\%$  (RSD%).

### Analytical Characteristics

Double-distilled water samples were used to estimate the precision of the measurements, the detection limit and the dynamic range of the method. Linear calibration curve and regression coefficient were obtained. As shown in Fig. 4a, increasing NAP concentrations leads to increase fluorescence intensities. A direct linear relationship between the response  $I_e$

**Table 4** ANOVA test results in double-distilled water and real samples spiked

| Spiked amount (ng/mL) | Samples       | Test for equal variances ( $\alpha = 0.05$ ) |                         | ANOVA Test for equal means ( $\alpha = 0.05$ ) |                     |
|-----------------------|---------------|--|-------------------------|--|---------------------|
|                       |               | P Value                                      | Result                  | P Value  | Result              |
| 40.0                  | DDW           | 0.988  | All variances are equal | 0.105  | All means are equal |
|                       | Mineral water |  |                         |  |                     |
|                       | Tap water     |  |                         |  |                     |
|                       | Plasma        |  |                         |  |                     |
| 100.0                 | DDW           | 0.860  | All variances are equal | 0.085  | All means are equal |
|                       | Mineral water |  |                         |  |                     |
|                       | Tap water     |  |                         |  |                     |
|                       | Plasma        |  |                         |  |                     |

(fluorescence intensity) and NAP concentrations was attained in 10–120 ng/mL and with regression equations of  $I_c = 6.386C_{\text{NAP}} + 47.021$  ( $R^2 = 0.9979$ ) (Fig. 4b). The limit of detection (LOD = 2.4 ng/mL) and the limit of quantitation (LOQ = 8.0 ng/mL) for NAP were quantified based on  $n = 9$  blank samples.

Table 2 compares the results obtained with the developed methods with other methods found in the literature. As the results show, the proposed method has a detection limit and linear range comparable to other methods. The greatest point of the present method is the simplicity, speed, and sensitivity of the method to NAP.

### Effect of Interferences & Real Samples Analysis

In similarity with most micro-extraction techniques, the extraction efficiency can be influenced by the matrix of the real specimens. Therefore, the effects of the matrix were investigated by comparing the results of the real samples with double-distilled water. The experiments were performed with plasma, tap water and mineral water samples to estimate the matrix effects and the applicability of the developed method, compared with double-distilled water samples. Experiments were performed on 15 mL of spiked NAP. The experiments were repeated 3 times. The results are presented in Table 3. As can be seen, recovery values and relative standard deviations indicate the sufficiency of the present method for measuring NAP in real samples.

Table 4 shows ANOVA test (Significant level  $\alpha = 0.05$ ) results that were used to compare the mean of the results between real samples and double-distilled water to ensure that the matrix effects of the real samples were not significant.

ANOVA test results are presented in double-distilled water and real spiked samples for 40.0 ng/mL NAP and 100.0 ng/mL NAP. The P value = 0.105 > 0.05 for NAP 40.0 ng/mL and P value = 0.085 > 0.05 for 100.0 ng/mL NAP showed that the mean values of the real samples and the double-distilled water samples had no significance at the 95% confidence level. This test showed that the real samples matrix does not have interference in the results and the developed method is applicable for the real samples.

### Conclusion

In this study, a sensitive method was developed based on the DLLME-SFO combination with spectrofluorimetry to measure very low amounts of NAP in water and plasma samples. This is a simple, fast and inexpensive method that has low toxicity because the very low solvent content is used. The proposed method has a good linear dynamic range, good detection limit and repeatability, and the matrix of the real samples does not affect the

results. These specifications, along with the inherent sensitivity of spectrofluorimetry, provide an effective and valid method for determining NAP in plasma and water samples. The application of central composite design results in the achievement of actual optimal values of effective parameters with a minimum number of experiments.

**Acknowledgements** The authors thank the chemical research laboratories in Central Tehran Branch, Islamic Azad University for their support in this study.

### Compliance with Ethical Standards

**Conflict of Interest** The author declares that there is no conflict of interest.

### References

- Gros M, Petrović M, Ginebreda A, Barceló D (2010) Removal of pharmaceuticals during wastewater treatment and environmental risk assessment using hazard indexes. *Environ Int* 36:15–26. <https://doi.org/10.1016/j.envint.2009.09.002>
- Yilmaz B, Sahin H, Erdem AF (2014) Determination of naproxen in human plasma by GC-MS. *J Sep Sci* 37:997–1003. <https://doi.org/10.1002/jssc.201301105>
- Rafiqi P, Yafthian MR, Haghghi B (2018) Magnetic nanofibrous polyaniline nanocomposite for solid-phase extraction of naproxen from biological samples prior to its spectrofluorimetric determination. *J Iran Chem Soc* 15:1209–1221. <https://doi.org/10.1007/s13738-018-1319-x>
- Sadrjavadi K, Shahlaei M, Bahrami G, Majnooni MB, Mohebbi M (2015) Comparison of correlation ranking and eigenvalue ranking unfolded principal component regression for direct determination of naproxen in human serum using excitation–emission matrix fluorescence spectroscopy. *J Iran Chem Soc* 12:967–977. <https://doi.org/10.1007/s13738-014-0559-7>
- Ayazi Z, Rafiqi P (2015) Preparation and application of a carbon nanotube reinforced polyamide-based stir bar for sorptive extraction of naproxen from biological samples prior to its spectrofluorimetric determination. *Anal Methods* 7:3200–3210. <https://doi.org/10.1039/C4AY02734E>
- Madrakian T, Ahmadi M, Afkhami A, Soleimani M (2013) Selective solid-phase extraction of naproxen drug from human urine samples using molecularly imprinted polymer-coated magnetic multi-walled carbon nanotubes prior to its spectrofluorimetric determination. *Analyst* 138:4542–4549. <https://doi.org/10.1039/C3AN00686G>
- Bagheri H, Roostaie A, Baktash MY (2014) A chitosan-poly pyrrole magnetic nanocomposite as  $\mu$ -sorbent for isolation of naproxen. *Anal Chim Acta* 816: 1–7. <https://doi.org/10.1016/j.aca.2014.01.028>
- Hajmohammadi MR, Hemmati M (2017) Vortex-assisted inverted dispersive liquid-liquid microextraction of naproxen from human plasma and its determination by high-performance liquid chromatography. *Iran J Chem Chem Eng* 36:107–114
- Muneer S, Muhammad IN, Abrar MA, Munir I, Kaukab I, Sagheer A, Zafar H, Sultana K (2017) High performance liquid chromatographic determination of naproxen in prepared pharmaceutical dosage form and human plasma and its application to pharmacokinetic

- study. *J Chromatogr Sep Tech* 8:369. <https://doi.org/10.4172/2157-7064.1000369>
10. Akhlaghi H, Ghorbani M, Afshar Lahoori N, Shams A, Seyedin O (2016) Preconcentration and determination of naproxen in water samples by functionalized multi-walled carbon nanotubes hollow fiber solid phase microextraction—HPLC. *J Anal Chem* 71:641–647. <https://doi.org/10.1134/S1061934816070091>
  11. Yilmaz B, Asci A, Erdem AF (2013) HPLC method for naproxen determination in human plasma and its application to a pharmacokinetic study in Turkey. *J Chromatogr Sci* 52:584–589. <https://doi.org/10.1093/chromsci/bmt080>
  12. Afzali M, Jahromi Z, Nekooie R (2018) Sensitive voltammetric method for the determination of naproxen at the surface of carbon nanofiber/gold/polyaniline nanocomposite modified carbon ionic liquid electrode. *Microchem J* 145:373–379. <https://doi.org/10.1016/j.microc.2018.10.046>
  13. Kianoush Sarhangzadeh K (2015) Application of multi wall carbon nanotube–graphene hybrid for voltammetric determination of naproxen. *J Iran Chem Soc* 12:2133–2140. <https://doi.org/10.1007/s13738-015-0690-0>
  14. Soltani N, NahidTavakkoli N, Zinat S, Mosavimanesh ZS, Davar F (2018) Electrochemical determination of naproxen in the presence of acetaminophen using a carbon paste electrode modified with activated carbon nanoparticles. *C R Chim* 21:54–60. <https://doi.org/10.1016/j.crci.2017.11.007>
  15. Rajabi HR, Zarezadeh A (2016) Development of a new chemically modified carbon paste electrode based on nano-sized molecular imprinted polymer for selective and sensitive determination of naproxen. *J. Mater. Sci. Mater. Electron* 27:10911–10920. <https://doi.org/10.1007/s10854-016-5202-1>
  16. Lenik J, Łyszczek R (2016) Functionalized  $\beta$ -cyclodextrin based potentiometric sensor for naproxen determination. *Mater Sci Eng C Mater Biol Appl* 61:149–157. <https://doi.org/10.1016/j.msec.2015.12.011>
  17. Tashkhourian J, Hemmateenejad B, Beigizadeh H, Hosseini-Sarvari M, Razmi Z (2014) ZnO nanoparticles and multiwalled carbon nanotubes modified carbon paste electrode for determination of naproxen using electrochemical techniques. *J Electroanal Chem* 714–715:103–108. <https://doi.org/10.1016/j.jelechem.2013.12.026>
  18. Rezaee M, Assadi Y, Milani Hosseini MR, Aghae E, Ahmadi F, Berijani S (2006) Determination of organic compounds in water using dispersive liquid-liquid microextraction. *J Chromatogr A* 1116(1–2):1–9. <https://doi.org/10.1016/j.chroma.2006.03.007>
  19. Šandrejová J, Campillo N, Pilar Viñas P, Andruch V (2016) Classification and terminology in dispersive liquid–liquid microextraction. *Microchem J* 127:184–186. <https://doi.org/10.1016/j.microc.2016.03.007>
  20. Mansour FR, Khairy MA (2017) Pharmaceutical and biomedical applications of dispersive liquid–liquid microextraction. *J. Chromatogr. B* 1061–1062:382–391. <https://doi.org/10.1016/j.jchromb.2017.07.055>
  21. Campillo N, Viñas P, Šandrejová J, Andruch V (2017) Ten years of dispersive liquid–liquid microextraction and derived techniques. *Appl Spectrosc Rev* 52:267–415. <https://doi.org/10.1080/05704928.2016.1224240>
  22. GilbertoPrimel E, SouzaCaldas S, CardosoMarube L, VenquiarutiEscarrone AL (2017) An overview of advances in dispersive liquid–liquid microextraction for the extraction of pesticides and emerging contaminants from environmental samples. *Trends Environ Anal* 14:1–18. <https://doi.org/10.1016/j.teac.2017.03.001>
  23. Wang Q, Chen R, Shatner W, Cao Y, Bai Y (2018) State-of-the-art on the technique of dispersive liquid-liquid microextraction. *Ultrason Sonochem* 51:369–377. <https://doi.org/10.1016/j.ultrsonch.2018.08.010>
  24. Leong MI, Huang SD (2008) Dispersive liquid-liquid microextraction method based on solidification of floating organic drop combined with gas chromatography with electron-capture or mass spectrometry detection. *J Chromatogr A* 1211(1–2):8–12. <https://doi.org/10.1016/j.chroma.2008.09.111>
  25. Viñas P, Campillo N, Andruch V (2015) Recent achievements in solidified floating organic drop microextraction. *Trac-Trend Anal Chem* 68:48–77. <https://doi.org/10.1016/j.trac.2015.02.005>
  26. Mansour FR, Danielson ND (2017) Solidification of floating organic droplet in dispersive liquid-liquid microextraction as a green analytical tool. *Talanta* 170:22–35. <https://doi.org/10.1016/j.talanta.2017.03.084>
  27. Ebrahimi-Najafabadi H, Leardi R, Jalali-Heravi M (2014) Experimental Design in Analytical Chemistry-Part I: theory. *J AOAC Int* 97:3–11. <https://doi.org/10.5740/jaoacint.SGEEbrahimi1>
  28. Ebrahimi-Najafabadi H, Leardi R, Jalali-Heravi M (2014) Experimental Design in Analytical Chemistry-Part II: applications. *J AOAC Int* 97:12–18. <https://doi.org/10.5740/jaoacint.SGEEbrahimi2>
  29. Brereton RG, Jansen J, Lopes J, Marini F, Pomerantsev A, Rodionova O, Roger JM, Walczak B, Tauler R (2017) Chemometrics in analytical chemistry—part I: history, experimental design and data analysis tools. *Anal Bioanal Chem* 409:5891–5899. <https://doi.org/10.1007/s00216-017-0517-1>
  30. Mousavi L, Tamiji Z, Khoshayand MR (2018) Applications and opportunities of experimental design for the dispersive liquid–liquid microextraction method - A review. *Talanta* 190:335–356. <https://doi.org/10.1016/j.talanta.2018.08.002>
  31. Montgomery DC (2017) Design and analysis of experiments, John Wiley & Sons, Inc. Hoboken, NJ

**Publisher's Note** Springer Nature remains neutral with regard to jurisdictional claims in published maps and institutional affiliations.